11

A VARIATION OF THE RIEMANN PROBLEM SOLUTION AND ITS APPLICATION TO IMPLICIT GODUNOV'S SCHEME

Igor MEN'SHOV and Yoshiaki NAKAMURA
Department of Aeronautical Engineering, Nagoya University, Nagoya 464-01, JAPAN

ABSTRACT

The present paper is devoted to investigate a variation of the exact Riemann problem (RP) solution with respect to a variation of the initial data. This variation may be written in the linear form by introducing variation matrices (VM) coupled with the corresponding side of initial discontinuity. It is shown that VM for the exact RP solution can be obtained in the explicit form for any initial data. Its application to the implicit Godunov scheme leads to the linear system of equations in Δ - form which is solved in two relaxation sweeps, backward and forward ones, by implementing LU approximate factorization. The advantage of the scheme obtained in such a way is large CFL number in calculating of super- and hypersonic flows around blunt body.

1.Introduction The idea of employing the exact solution of RP in numerical methods was developed by Godunov [1], which produced a wide class of numerical schemes referred to as Godunov's type. Originally it was an explicit finite volume method (FVM), where the numercal flux on cell edge is equal to the value of differential flux in the exact solution of the RP with the initial data equal to the mean values of the state parameter vectors in the cells adjacent to the edge.

The time step for any explicit scheme is restricted by the Courant-Friedrichs-Lewy (CFL) condition, which requires that the domain of dependence in numerical scheme must at least include the domain of dependence in differrential equations. In the case of the explicit Godunov method the time step must be such that the trajectories of the discontinuities which appear as a result of an initial discontinuity decomposition do not intersect during the time step.

This time step restriction can be removed by the introduction of implicit scheme. Generally, the implicit scheme is nonlinear with respect to new time level. To solve this numerically, either iterative method or linearization of the original numerical scheme is used [2].

The latter approach developed in [3,4] for gas dynamic equations is based on the linearization of differential flux, the splitting Jacobian matrix into positive and negative parts, and the upwind finite difference approximation. The system of equations in Δ-form thus obtained can be approximately factorized into the product of two subsystems with block bidiagonal matrices in one-dimensional case. In multi-dimensional case it leads to the alternating direction implicit (ADI) procedure [5]. The ADI scheme is unconditionally stable in two dimensions. However, it is well known [6] that the corresponding scheme in Δ-form is unconditionally unstable in three dimensions.

An alternative approximate factorization of the implicit scheme, which was proposed in [7] and developed in [8,9], is lower-upper (LU) approximate factorization. It is stable in any space dimension, and in fact, is reduced to the symmetric Gausse-Seidel relaxation method for the unfactored implicit scheme with a single subiteration.

The present method belongs to the same family. However, it comes from an attempt to directly consider the linearization of the implicit FVM, that is, the linearization of the numerical flux in FVM instead of differential flux. This approach seems to be attractive because it can be easily extended to unstructured grid.

In this paper the Godunov method is employed for flux evaluation. First, the variation matrices for the exact Riemann problem solution are constructed in the explicit form for any initial data. Then, using these matrices the linear Δ–form of the implicit FVM and its approximate LU factorization are derived for arbitrary grid. Finally, the implicit scheme thus obtained is applied to supersonic and hypersonic flows with strong shock wave.

2.Governing equations Let ρ, u_k, E, H, p be the density, the Cartesian velocity components, the total energy, the total enthalpy, and the pressure. Then, the three-dimensional Euler equations can be written as

$$\frac{\partial \vec{q}}{\partial t} + \frac{\partial \vec{F}_k(\vec{q})}{\partial x_k} = 0 \qquad (1)$$

where $\vec{q}$ is the solution vector and $\vec{F}_k$ are differential flux vectors:

$$\vec{q} = \begin{bmatrix} \rho \\ \rho u_1 \\ \rho u_2 \\ \rho u_3 \\ \rho E \end{bmatrix}; \quad \vec{F}_k = \begin{bmatrix} \rho u_k \\ \rho u_1 u_k + \delta_{1,k} p \\ \rho u_2 u_k + \delta_{2,k} p \\ \rho u_3 u_k + \delta_{3,k} p \\ \rho u_k H \end{bmatrix} \qquad (2)$$

x_k is Cartesian coordinates, and the equation of state is given for a perfect gas as

$$p = (\gamma - 1)\rho(E - \sum_{k=1}^{3} u_k^2) \qquad (3)$$

where γ is the ratio of specific heats.

3. <u>Implicit finite volume approximation</u> Use of FVM for space discretization can handle arbitrary geometries and computational grids, and helps to avoid problems with metric singularities that are usually associated with the finite difference method. We consider a computational grid, where the computational domain is divided into nonoverlapping cells. Then the finite volume scheme is derived by integrating eq. (1) in each cell, and transforming cell volume integral to cell boundary integral:

$$\omega_i(\vec{q}_i^{n+1} - \vec{q}_i^n) = -(1-\beta)\Delta t \sum_\sigma s_\sigma \vec{F}_\sigma^n - \beta \Delta t \sum_\sigma s_\sigma \vec{F}_\sigma^{n+1} \quad (4)$$

where $\vec{q}_i$ is the cell average parameter vector, ω_i is the cell volume, Δt is time step, β is parameter ($0< \beta<1$), and S_σ is the area of cell interface. Here n denotes the time level, and σ the cell interface. $\vec{F}_\sigma$ is so-called numerical flux which is equal to cell interface average value with regard to the projection of the diferential flux onto exterior normal.

The parameter β determines the specific time differencing approximation used. The scheme with β =0 is explicit, β =1 is full implicit , and β =0.5 is of second order of approximation in time.

The numerical flux can be written in general form. If we introduce the local cell interface orthonormal basis $\vec{n} = (n_1, n_2, n_3)$, $\vec{k} = (k_1, k_2, k_3)$, $\vec{l} = (l_1, l_2, l_3)$, where $\vec{n}$ is the exterior normal to cell interface, and local one-dimensional flux vector $\vec{F}$:

$$\vec{F} = \begin{bmatrix} \rho u \\ \rho u^2 + p \\ \rho v u \\ \rho w u \\ \rho u H \end{bmatrix} \qquad (5)$$

where (u,v,w) are the components of the velocity vector in this basis, the numerical flux $\vec{F}_\sigma$ can be written in the general form:

$$\vec{F}_\sigma = T_\sigma \vec{F}$$

where T_σ is the transforming matrix:

$$T_\sigma = \begin{bmatrix} 1 & 0 & 0 & 0 & 0 \\ 0 & n_1 & n_2 & n_3 & 0 \\ 0 & k_1 & k_2 & k_3 & 0 \\ 0 & l_1 & l_2 & l_3 & 0 \\ 0 & 0 & 0 & 0 & 1 \end{bmatrix} \qquad (6)$$

The flux vector $\vec{F}$ is usually defined by the values of parameter vectors in the two cells adjacent to a cell interface:

$$\vec{F} = \vec{F}(\vec{Q}_i, \vec{Q}_{\sigma(i)}); \quad \vec{Q} = T_\sigma^{-1} \vec{q} \qquad (7)$$

where $\sigma(i)$ denotes the cell, which adjoins the i-cell through the cell interface σ.

In Godunov's scheme we have

$$\vec{F} = \vec{F}(\vec{Q}_\sigma); \quad \vec{Q}_\sigma = \vec{Q}^R(0, \vec{Q}_i, \vec{Q}_{\sigma(i)}) \qquad (8)$$

Here $\vec{Q}^R$ denotes the exact solution of the RP.

In flux vector splitting schemes, FVS, the flux vector is given in the form:

$$\vec{F} = \vec{F}^+(\vec{Q}_i) + \vec{F}^-(\vec{Q}_{\sigma(i)}) \qquad (9)$$

where $\vec{F}^+$ and $\vec{F}^-$ are positive and negative parts of the differential flux [4,10].

4. <u>Linearization and LU approximate factorization</u> The implicit scheme in the form of eq. (4) is too expensive to calculate since it requires the solution of coupled nonlinear equations at each time step. A simple approach to the treatment of the non-linearity, taking the advantage of the fully implicit scheme, is local linearization of the non-linear terms in eq. (4), i.e. the flux vector (Newton method). The Newton method is defined in the following way.

Let the increment of a vector Φ at the time level n be

$$\Delta\Phi = \Phi^{n+1} - \Phi^n$$

Taking into account that the flux vector $\vec{F}$ of eq.(7) can be expanded as

$$\vec{F}_\sigma^{n+1} = \vec{F}_\sigma^n + \mu_\sigma^1 \Delta\vec{q}_i + \mu_\sigma^2 \Delta\vec{q}_{\sigma(i)} + O(\|\Delta\vec{q}_i\|^2, \|\Delta\vec{q}_{\sigma(i)}\|^2)$$

and dropping terms of the second and higher order, it yields

$$\left(\omega_i I + \beta\Delta t \sum_\sigma S_\sigma \mu_\sigma^{(1)}\right)\Delta\vec{q}_i + \beta\Delta t \sum_\sigma S_\sigma \mu_\sigma^{(2)} \Delta\vec{q}_{\sigma(i)} = -\Delta t \vec{r}_i \quad (10)$$

where $\vec{r}_i$ is the residual

$$\vec{r}_i = \sum_\sigma S_\sigma \vec{F}_\sigma^n$$

If β=0.5, the scheme is second-order accurate in time, while for other values of β it is of first order.

The variation matrices $\mu_\sigma^{(1,2)}$ are defined in general form as

$$\mu_\sigma^{(1)} = T_\sigma^{-1} \frac{\partial\vec{F}}{\partial\vec{Q}_i} T_\sigma; \qquad \mu_\sigma^{(2)} = T_\sigma^{-1} \frac{\partial\vec{F}}{\partial\vec{Q}_{\sigma(i)}} T_\sigma \qquad (11)$$

for flux (7) with two arguments.

In the case of Godunov's flux, the derivatives in eq.(11) can be written by the Jacobian matrix A in the exact RP solution:

$$\frac{\partial \vec{F}}{\partial \vec{Q}_k} = A\left(\vec{Q}_\sigma\right)\frac{\partial \vec{Q}^R}{\partial \vec{Q}_k}; \quad k = i, \quad \sigma(i) \qquad (12)$$

where $\partial \vec{Q}^R / \partial \vec{Q}_k$ are variation matrices of the exact RP solution, which will be derived below.

In FVS, the variation matrices are obtained directly from eq.(9) as follows:

$$\mu_\sigma^{(1)} = T_\sigma^{-1}\frac{\partial \vec{F}^+}{\partial \vec{Q}_i}T_\sigma; \qquad \mu_\sigma^{(2)} = T_\sigma^{-1}\frac{\partial \vec{F}^-}{\partial \vec{Q}_{\sigma(i)}}T_\sigma$$

The implicit scheme (10) produces a large block band matrix, which can be inverted only by performing many operations. In [7] an idea of LU approximate factorization was proposed for the implicit scheme on regular grids, that is unconditionally stable in any number of space dimension, and leads to the system of equations with sparse triangular matrix. For an arbitrary grid, following this idea we can introduce LU decomposition of eq. (10) by separating the summation in it into two parts:

$$\sum_\sigma\left(S_\sigma\mu_\sigma^{(1)}\Delta\vec{q}_i + S_\sigma\mu_\sigma^{(2)}\Delta\vec{q}_{\sigma(i)}\right) = \sum_\sigma S_\sigma\mu_\sigma^-\Delta\vec{q}_\sigma^- + \sum_\sigma S_\sigma\mu_\sigma^+\Delta\vec{q}_\sigma^+$$

where

$$\mu_\sigma^-\Delta\vec{q}_\sigma^- = \begin{cases}\mu_\sigma^{(1)}\Delta\vec{q}_i, & \text{if } i < \sigma(i)\\ \mu_\sigma^{(2)}\Delta\vec{q}_{\sigma(i)}, & \text{if } i > \sigma(i)\end{cases}$$

$$\mu_\sigma^+\Delta\vec{q}_\sigma^+ = \begin{cases}\mu_\sigma^{(2)}\Delta\vec{q}_{\sigma(i)}, & \text{if } i < \sigma(i)\\ \mu_\sigma^{(1)}\Delta\vec{q}_i, & \text{if } i > \sigma(i)\end{cases}$$

and simulating (10) with backward and forward relaxation sweeps. Then LU factorized scheme can be written in two steps as:

$$\omega_i\Delta\vec{q}_i^* + \beta\Delta t\sum_\sigma S_\sigma\mu_\sigma^-\Delta\vec{q}_\sigma^{*-} = -\Delta t\vec{r}_i \qquad (13)$$

$$\omega_i\Delta\vec{q}_i + \beta\Delta t\sum_\sigma S_\sigma\mu_\sigma^+\Delta\vec{q}_\sigma^+ = \omega_i\Delta\vec{q}_i^*$$

The system of equations (13) is solved in two steps. First, the first system is solved as the number of cell increases (direct sweep). Then, in the opposite sweep, where the number of cell decreases, the final increment is defined by solving the second system. The latter is used to obtain the parameter vector on the new time level. In each sweep one needs to invert a sparse triangular matrix. In practice it reduces to inversion of 5x5 matrix in three dimensions and 4x4 matrix in two dimensions for each computational cell, and can be perfomed efficiently without any large storage. Equations (13) are actually a explicit scheme, which defines sequentially the increments in cells during the forward and backward sweeps of computational grid.

5. Variation matrices for the exact RP solution The RP for gas dynamic equations can be considered as Cauchy problem:

$$\frac{\partial \vec{Q}}{\partial t} + \frac{\partial \vec{F}(\vec{Q})}{\partial x} = 0$$

with initial data at t=0

$$\vec{Q} = \begin{cases}\vec{Q}_l & x < 0\\ \vec{Q}_r & x > 0\end{cases} \qquad (14)$$

where t and x are time and space coordinates, $\vec{Q}$ and $\vec{F}$ are defined in eq.(2), and $\vec{Q}_l$ and $\vec{Q}_r$ are constant.

This problem has a unique solution under any initial data. The solution is a piecewise analytical function $\vec{Q}^{(R)}$, which depends on the initial data and parameter λ=x/t [11]:

$$\vec{Q}(\lambda) = \vec{Q}^{(R)}\left(\lambda, \vec{Q}_l, \vec{Q}_r\right)$$

The number of singular points of this function is strictly limited. It must be less than 5 in general case. Moreover, their physical types (or wave pattern, because the singular points represent the velocities of several discontinuities originated from the breake-up of an initial discontinuity) have always a certain order. That is, the contact discontinuity (CD) arises. It separates the gas which was initially on the left (x<0) from one on the right (x>0). A constant flow domains (contact zones) in both sides of CD have the same pressure and velocity. The contact zone might be separated from an unperturbed zone by a shock wave, or a fan of rarefaction waves (RW). In the domain of RW the solution is described by the relations:

$$\vec{Q}^{(R)}(\lambda): \quad u \pm a - \lambda = 0; \; cu' \mp p' = 0; \; s' = v' = w' = 0 \qquad (15)$$

where a is the sound velocity, c=ρa, s is the entropy, and the prime denotes the derivative with regard to λ. Except for the RW zone, the solution does not depend on λ.

Considering a variation of the initial data

$$\vec{Q}_l \to \vec{Q}_l + \delta\vec{Q}_l; \qquad \vec{Q}_r \to \vec{Q}_r + \delta\vec{Q}_r$$

we are concerned with the first variation of the solution

$$\delta\vec{Q} = M_l\delta\vec{Q}_l + M_r\delta\vec{Q}_r$$

where the variation matrices (VM) $M_{l,r}$ are defined as

$$M_{l,r} = M_{l,r}\left(\lambda, \vec{Q}^{(R)}\right) = \frac{\partial \vec{Q}^{(R)}}{\partial \vec{Q}_{l,r}}$$

The problem is to find VM for any arbitrary initial data. It is evident that $M_{l,r}$ are piecewise analytical functions that have the same singular points as the solution $\vec{Q}^{(R)}$, and are constant with respect to λ everywhere but the zone of RW.

In what follows, it is convenient to introduce the vector $\vec{U} = (u, p, s, v, w)^T$ instead of the vector $\vec{Q}$. The corresponding VM is denoted by μ.

Evidently, we have for the left unperturbed zone:

$$\mu_l = I; \quad \mu_r = 0$$

and for the right one

$$\mu_l = 0; \quad \mu_r = I$$

where I is the identity matrix.

Varying (15), we can obtain the VM in the zone of RW in the form:

$$\mu_i = \mu_{RW} = \begin{bmatrix} \alpha & \mp\frac{\alpha}{c_i} & 0 & 0 & 0 \\ \mp\beta & \frac{\beta c}{c_i} & \frac{a\beta}{2\alpha s} & 0 & 0 \\ 0 & 0 & 1 & 0 & 0 \\ 0 & 0 & 0 & 1 & 0 \\ 0 & 0 & 0 & 0 & 1 \end{bmatrix}; \quad i = l, r \quad (16)$$

where

$$\alpha = \frac{\gamma-1}{\gamma+1}; \quad \beta = \frac{2}{\gamma+1}$$

and the upper and lower signs correspond to the right and left RW, respectively.

In the contact zone, VM are constant and must be defined by considering conjugate relations between the variations at the internal characteristic of the RW or at the shock wave.

Analysing these relations, we can derive that the variations in the contact zones on the left and on the right with respect to CD in all possible cases are written in the form with an indeterminacy of one arbitrary constant C_i:

$$\delta\vec{U} = N^{(i)}\delta U_i + \vec{m}^{(i)} C_i \ , \quad i = l, r \qquad (17)$$

where $N^{(i)}$ and $\vec{m}^{(i)}$ are matrix and vector. It is natural to call them variation matrix and variation vector of contact zone, and they can be written out in the explicit form. In the case when the contact and unperturbed zones are separated by RW, they have the form:

$$N^i = \begin{bmatrix} 0 & 0 & 0 & 0 & 0 \\ \mp c & \frac{c}{c_i} & \frac{c(a-a_i)}{(\gamma-1)s} & 0 & 0 \\ 0 & 0 & 1 & 0 & 0 \\ 0 & 0 & 0 & 1 & 0 \\ 0 & 0 & 0 & 0 & 1 \end{bmatrix}; \quad \vec{m}^i = \begin{bmatrix} 1 \\ \pm c \\ 0 \\ 0 \\ 0 \end{bmatrix}; \quad i = l, r \quad (18)$$

For the case of shock wave they are

$$N^i = \begin{bmatrix} 1 & \frac{1+M_i^2}{m_i} + \chi_2 & -\sigma_i m_i T_i - \chi_3 & 0 & 0 \\ 0 & -m_i\chi_2 & m_i\chi_3 & 0 & 0 \\ 0 & -\frac{\Delta}{m_i T} & \frac{T_i}{T} & 0 & 0 \\ 0 & 0 & 0 & 1 & 0 \\ 0 & 0 & 0 & 0 & 1 \end{bmatrix}; \vec{m}^i = \begin{bmatrix} -1-\chi_1 \\ \chi_1 m_i \\ \frac{\Delta}{T} \\ 0 \\ 0 \end{bmatrix}$$

where

$$m_i = \rho_i(u_i - D_{sh}); \quad \Delta = u - u_i; \quad M_i = m_i / c_i \ ; \qquad (19)$$

$$\chi_1 = \frac{2 + m_i\sigma\Delta}{M^2 - 1}; \quad \chi_2 = \frac{1 + M_i^2 + m_i\sigma\Delta}{m_i(M^2-1)}; \quad \chi_3 = m_i T_i \frac{\sigma + \sigma_i}{M^2 - 1}$$

$$T = -\frac{a^2}{(\gamma-1)s}; \quad \sigma = \frac{\gamma-1}{\gamma P}; \quad s = \rho \cdot P^{-1/\gamma}$$

and D_{sh} is the velocity of shock wave.

To determine two constants C_l and C_r in eq.(17), there are two conjugate relations on the CD

$$[\delta u]=0, \quad [\delta p]=0$$

This completes the solution for the variation of the exact RP solution.

The final result can be expressed in the compact form if we introduce proper and associated values depending on the value of the parameter λ. For example, if the value of λ is such that it corresponds to the left side of CD, then the left side parameters are proper but right side ones are associated, and vice versa. Denoting the associated values by asterisk , and the initial data by circle, the variation of the exact RP solution can be written as

$$\delta\vec{U} = \mu\delta\vec{U}_0 + \mu^*\delta\vec{U}_0^*$$

where

a) $\mu = I, \quad \mu^* = 0$ in the unperturbed zone;

b) $\mu = \mu_{RW}, \ \mu^* = 0$ in the RW zone;

c) $\mu = N - \vec{m} \circ \vec{k}^*; \ \mu^* = \vec{m} \circ \vec{n}^*$ in the contact zone;

$$\vec{n} = \frac{m_2\vec{N}_1 - m_1\vec{N}_2}{m_2 m_1^* - m_1 m_2^*}; \qquad \vec{k} = \frac{m_2\vec{N}_1^* - m_1\vec{N}_2^*}{m_2 m_1^* - m_1 m_2^*}$$

Here μ_{RW} , N, and $\vec{m}$ are defined in eq.(17), (18), and (19), respectively for RW and schock wave; the vectors $\vec{N}_{1,2}$ are the first and second row of the matrix N, $m_{1,2}$ are the first and second components of the vector $\vec{m}$.

6. Numerical results Two dimensional calculations of inviscid hypersonic flows around a cylinder have been performed to verify the implicit Godunov scheme. The freestream Mach numbers of 6 and 20 are used. Comparisons are made between explicit (scheme SE) and implicit (scheme SI) Godunov's scheme. Three types of the grid are considered: a coarse grid of 40x15 with 40 cells along the cylinder surface and 15 cells normal to the surface, a middle grid of 30x80, and a fine grid of 60x160. The CFL number is equal to 1 for SE scheme , while for SI scheme it is varied from 1 at the beginnig to 100 after 30-50 iterations from impulsive start.

Convergence rate is evaluated by the value of the residual of density in L_∞ norm (Res) as a function of the number of iterations. Implicit mirror wall condition is imposed at the cylinder surface. The upper part of the flow domain is shown in the figures below.

The first case considered is a supersonic flow at

M=6. The density contours (Fig.1) given by implicit and explicit schemes on the grid of 60x160 (Fig.2) are identical. Therefore, the implicit Godunov scheme yields a steady state solution that is independent of time step Δt . For this case, the convergence rate presented in Fig.3 shows that the residual of the SI scheme drops more than 3 times faster than one in the SE scheme.

The same tendency is observed if we use more coarse grids as shown in Figs.4 and 5. Thus, to get the value of the residual of 10^{-10} by the SE scheme using 15x40 mesh needs approximately the same number of time step as the SI scheme on 60x160 mesh.

A hypersonic flow at M=20 has been taken up as a case which is not appropriate for Godunov's type schemes. In this case a numerical instability in capturing a strong shock wave, called "carbuncle phenomenon" [12], can appear in multi-dimensional computations.

As a result of this phenomenon, an ambiguous numerical solution may be produced by Godunov's scheme. It can be seen in Fig.6, where some numerical results at M=20 by explicit Godunov's scheme are presented. These calculations have been carried out by the same numerical code with CFL number of 1, and the residual of 10^{-10} . have been achieved. The carbuncle phenomenon doesn't develop on a coarse grid, whereas it does on a fine grid of 30x80 .

The convergence history for M=20 is presented in Fig.7. When the carbuncle phenomenon doesn't appear (Fig.7 a), the relation between convergence rates for SE and SI schemes is the same as that of M=6. Otherwise, the carbuncle phenomenon causes an oscillating slow convergence in the SE scheme, and doesn't affect the convergence in SI scheme (Figs.7b and 7c). The numerical solution in this case is incorrect near the stagnation stream line. However, it can be removed by introducing a dissipative mechanism to stabilize the shock wave [13].

7. Conclusions A variation of the exact Riemann problem solution has been considered in the present paper. It has been shown that the variation matrices can be derived in the explicit form for any arbitrary initial data and used to linearize numerical fluxes in the implicit Godunov method. The linear system of equations written in the Δ-form has been factorized in approximate LU form, which is relaxed in backward and forward sweeps for arbitrary computational grids. The results of some numerical experiments with the implicit scheme thus obtained show more capability and higher convergence rate to a steady state solution than explicit scheme. The general approach considered herein, based on the numerical flux linearization in implicit FVM, seems to be attractive because it can be easily extended to unstructured grid and the N.-S. equations.

Acknowledgment

This work was supported in part by the Russian Fund of Fundamental Researches under Grant N 93-012-516.

References

[1] Godunov, S.K., A Finite Difference Method for the Numerical Computation of Discontinuous Solutions of the Equations of Fluid Dynamics, Mat.Sb., 47, 3, pp.357-393, 1959.

[2] Yanenko, N.N., The Method of Fractional Steps for Solution Multi-Dimensional Problems of Mathematical Physics, M.: Nauka, 1967 (in Russian).

[3] Briley, W.R., and McDonald, H., On the Structure and Use of Linearized Block Implicit Schemes, J.Comp.Phys., 34, 1, pp.54-73, 1980.

[4] Steger, J.L., and Warming, R.F., Flux Vector Splitting of the Inviscid Gasdynamic Equations with Application to Finite Difference Methods, J.Comp.Phys., 40, 2, pp.263-293, 1976.

[5] Peaceman, D.W., and Rachford, H.H., The Numerical Solution of Parabolic and Elliptic Differential Equations, SIAM, No 3, pp. 28-41, 1955.

[6] Hirsch, C., Numerical Computation of Internal and External Flows, v.I, A Wiley - Interscience Publication, p.439, 1991.

[7] Jameson, A., and Turkel, E., Implicit Schemes and LU Decompositions, Mathematics of Computation, 37, 156, pp. 385-397, 1981.

[8] Jameson, A., and Yoon, S., Multigrid Solution of the Euler Equations Using Implicit Schemes, AIAA, 24, pp.1737-1743, 1986.

[9] Jameson, A., and Yoon, S., Louwer-Upper Implicit Schemes with Multiple Grids for the Euler Equations, AIAA , 25, pp.929-935, 1987.

[10] Van Leer., B., Flux Vector Splitting for the Euler Equations, Lecture notes in Physics, Berlin: Springer Verlag, 170, pp.507-512, 1982

[11] Kochin, N.E., Collected Papers, 2, Moscow: Izd.Akad.Nauk SSSR, pp.5-42, 1949 (in Russian).

[12] Quirk, J.J., A Contribution to the Greate Riemann Solver Debate, ICASE Report N 92-64, 1992.

[13] Wada, Y., Lion, M.S., A Flux Splitting Scheme with High Resolution and Robustness for Discontinuities, AIAA paper 94-0083, 1994.

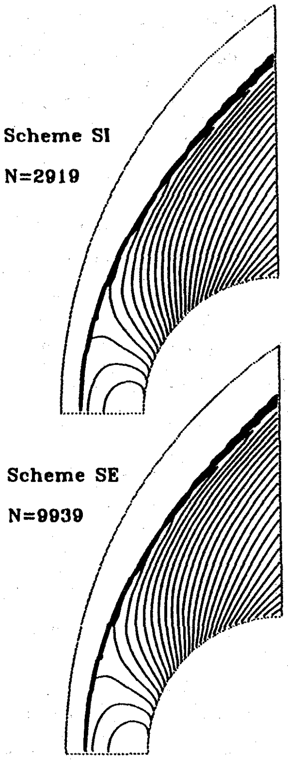

Fig.1 Density contours: M=6,and mesh 60x160

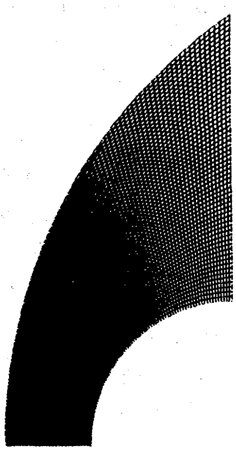

Fig.2 60x160 mesh

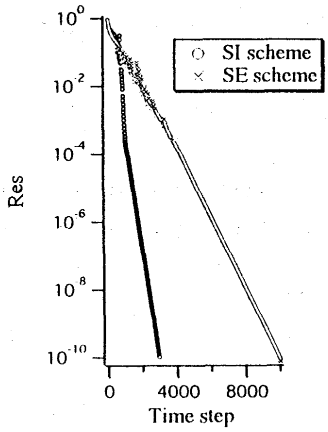

Fig.3 Convergence in residual (60x160 mesh)

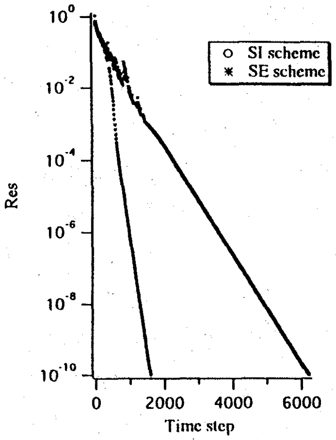

Fig.4 Convergence in residual (30x80 mesh)

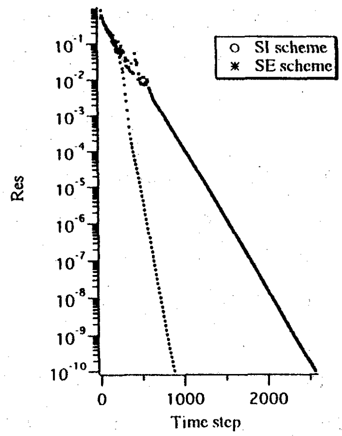

Fig.5 Convergence in residual (15x40 mesh)

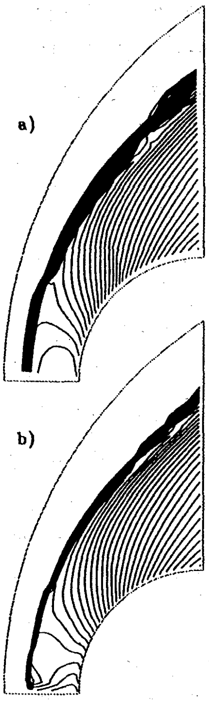

Fig.6 Density contours. M=20 and mesh: a)15x40, b)30x80

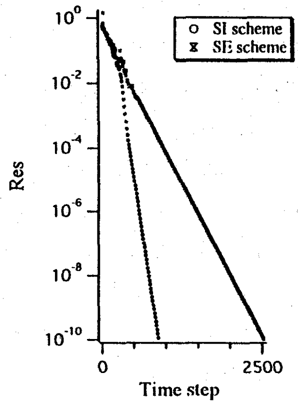

a) 15x40 mesh

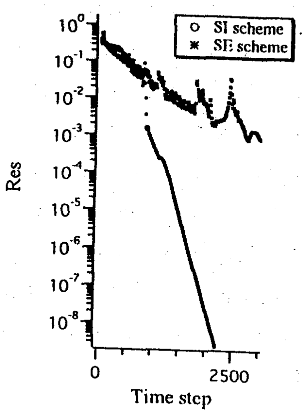

b) 30x80 mesh

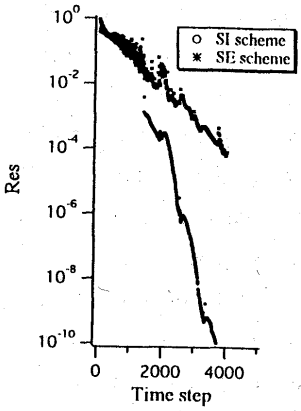

c) 60x160 mesh

Fig.7 Convergence in residual: M=20